DOI:
10.1007/s00330-014-3445-x

Document Version
Peer reviewed version

This is the author accepted manuscript version of Eur Radiol DOI 10.1007/s00330-014-3445-x

A 16-channel MR coil for simultaneous PET/MR imaging in breast cancer

Isabel Dregely[1], Titus Lanz[2], Stephan Metz[3], Matthias F. Mueller[2], Marika Kuschan[1,5], Manoj Nimbalkar[1], Ralph A. Bundschuh[1,4], Sibylle I. Ziegler[1], Axel Haase[5], Stephan G. Nekolla[1*], Markus Schwaiger[1*]

[1] Nuklearmedizinische Klinik, Klinikum rechts der Isar der Technischen Universität München, Germany
[2] Rapid Biomedical GmbH, Rimpar, Germany
[3] Institut für diagnostische und interventionelle Radiologie, Klinikum rechts der Isar der Technischen Universität München, Germany
[4] Nuklearmedizinische Klinik, Universitätsklinikum Bonn, Germany
[5] IMETUM, Technische Universität München, Germany
* Both senior authors contributed equally

Corresponding author:
Isabel Dregely, PhD
Department of Radiological Sciences
300 UCLA Medical Plaza, Suite B109
Los Angeles, CA 90095
Phone: +1 626 241 2232
Fax: +1 310 825 9118
Email: isabel.dregely@gmail.com

Financial support: The PET/MR system used for this study was funded through the "Deutsche Forschungsgemeinschaft (DFG) Grossgeräteinitiative 2010". Titus Lanz and Matthias F. Mueller are employees of Rapid Biomedical GmbH, Rimpar, Germany. The Technical University of Munich and Rapid Biomedical GmbH, Rimpar, Germany received research funding from the „Bundesministerium für Wirtschaft und Technologie (BMWi)". This work was supported in part by the „Bundesministerium für Wirtschaft und Technologie (BMWi)" and a research grant from Siemens Healthcare.

Foot line: Breast MR coil for simultaneous PET/MR

This is the author accepted manuscript version of Eur Radiol DOI 10.1007/s00330-014-3445-x

ABSTRACT

Objectives

To implement and evaluate a dedicated receive array coil for simultaneous PET/MR in breast cancer.

Methods

The 16 receiver channel coil design was optimized for simultaneous PET/MR. To assess MR performance, signal-to-noise ratio, parallel imaging capability and image quality was evaluated in phantoms, volunteers and patients and compared to clinical standard protocols. For PET evaluation, quantitative ^{18}F-FDG PET scans of phantoms and seven patients (14 lesions) were compared to scans without coil. In PET image reconstruction, a CT-based template of the coil was combined with the MR-acquired attenuation correction (AC) map of the phantom / patient.

Results

MR image quality was comparable to clinical MR-only exams. PET evaluation in phantoms showed regionally varying SUV underestimation (mean 22%) due to attenuation caused by the coil. This was improved by implementing the CT-based coil template in the AC (< 2% SUV underestimation). Patient data showed that including the coil in the AC increased SUV values in lesions (21% ± 9 %).

Conclusions

Using a dedicated PET/MR breast coil, state-of-the-art MRI was possible. In PET accurate quantification and image homogeneity could be achieved, if a CT-template of this coil was included in the attenuation correction for PET image reconstruction.

Keywords

Magnetic Resonance Imaging, Positron-Emission Tomography, Breast cancer, Bilateral breast imaging, RF coil array

Key Points

- State-of-the-art breast MRI using a dedicated PET/MR breast coil is feasible.
- A multi-channel design facilitates shorter MR acquisition times through parallel imaging.
- The MR coil inside a simultaneous PET/MR system causes PET photon attenuation.
- Including a coil CT-template in PET image reconstruction, accurate quantification is recovered.

INTRODUCTION

Recent developments in hardware technology [1] have enabled simultaneous PET/MR systems [2-4]. Although successfully applied in many oncologic applications, simultaneous PET/MR in breast cancer has so far been delayed due to the need for a dedicated breast coil, which enables prone positioning and achieves high image quality, as a precondition for state-of-the-art breast MRI [5]. However, the presence of MR related hardware, such as a breast coil, in the PET field-of-view (FOV) causes significant attenuation of the 511 keV annihilation photons, therefore hampering PET image quality [6]. Studies found, that the presence of MR head coils, which contain a substantial amount of plastic housing material, lead to 13-19% underestimation of PET activity concentration, if not accounted for during image reconstruction [7]. The attenuation effects for “lighter” or more “transparent” MR surface coils were only 4% overall, but up to 10-15% closer to the coil surface [8]. These results demonstrate that disregarding the presence of MR coils leads to substantial regional bias in PET quantification and illustrate the importance of accurate implementation of methodology for MR coil attenuation correction (AC) in simultaneous PET/MR applications. Even though MR coils are invisible in the conventional MR-acquired AC maps, it was shown that coil AC can be successfully implemented using a CT-based template of the coil, which is fused with the MR-based AC-map of the patient [6,9,10].

In this work we describe design and implementation of a prototype 16-channel MR coil specifically developed for simultaneous PET/MR in breast cancer. Our goal was to validate that state-of-the-art MR image quality can be achieved, while simultaneously PET image quality and accurate quantification is not restricted. Results of this study should provide the methodological validation for future clinical studies of simultaneous PET/MR in breast cancer.

MATERIALS AND METHODS

PET/MR coil design

The design of the dedicated PET/MR breast coil was based on a MR-only breast coil [11]. It allowed for patient prone positioning. 16 coil elements were arranged around two cylinders. In order to minimize attenuation of PET photons due to high absorbing components along the line-of-response (LOR), electronics with high "component density" such as preamplifiers were moved away from the imaging FOV (Fig. 1a,b).

Phantom studies

All PET/MR imaging studies were performed in a simultaneous PET/MR system (Biograph mMR, Siemens Healthcare, Erlangen, Germany). For phantom studies, two 1-liter plastic bottles were filled with Gd-DTPA doped water and placed in the coil. For PET imaging experiments 75 MBq of ^{18}F-FDG was homogeneously diluted in each bottle. A rather large activity was used to accurately characterize the effect of the coil on PET images. The MR performance measurements of the dedicated PET/MR coil were compared to a standard commercially available MR-only breast coil (Rapid Biomedical GmbH, Rimpar, Germany, [11]). A 2D spoiled gradient echo sequence of the phantom bottles was acquired to generate signal-to-noise ratio (SNR) maps. The sequence was repeated with no radio frequency (RF) excitation power (flip angle 0°) for a noise measurement to assess the noise correlation of the receiver channels and calculate the SNR maps [12]. Both measurements were done for the MR-only coil as well.

For PET performance measurements, 4 min static emission scans of the two ^{18}F-FDG doped water bottles were acquired. For a quantitative measure of tracer concentration, an AC-map of the phantoms was obtained by using the system's implemented automatic tissue segmentation algorithm of a Dixon MR-acquisition [13]. To evaluate PET photon attenuation due to the coil presence in the PET FOV, five PET measurements were obtained: (i) without any coil present (reference data), (ii) with the prototype PET/MR coil, (iii) with only the PET/MR coil housing material, (iv) with the commercially available 16-ch MR-only coil [11] and (v) with a 7-ch MR-only coil (commercially available biopsy breast array coil, InVivo Corporation, Gainesville, Florida, USA) present.

Volunteer and patient studies

Two female volunteers were imaged after signed informed consent was obtained for MR evaluation without contrast agent administration. SNR maps as described above were acquired in one volunteer. To assess parallel MRI performance of the 16-ch PET/MR coil, a clinical routine breast MRI sequence (axial T2-weighted 2D-turbo spin echo (TSE) sequence with TR/TE 4650 ms / 119 ms, BW 221 Hz/pixel, avg 2, matrix 384 x 384, pix spacing 1.0 x 1.0 mm^2, acceleration factor 3, slice thickness 2 mm, 90 slices) was acquired with acceleration factor (AF) 3 (TA 7 min 23 s) and 7 (TA 4 min 17 s) in the second volunteer.

Seven patients (age mean ± SD = 49 ± 17) years) with breast cancer underwent a PET/MR examination on the integrated whole-body scanner using the PET/MR breast coil after their clinical PET/CT scan. All patients gave informed consent, and the approval of the institutional review board and the radiation protection authorities had been obtained. Patients were injected with ^{18}F-FDG radiotracer (dose mean ± SD = 344 ±

52 MBq) and imaged in the simultaneous PET/MR scanner 101-175 min p.i. in prone positioning using the dedicated breast coil. The imaging protocol included a MR Dixon acquisition in coronal orientation (TR/TE 3.6 ms / 2.46 ms, FA 10°, pixel bandwidth 965 Hz/pixel, TA 30 s, matrix 126 x 192 x 127, pixel spacing 2.3 x 2.3 x 2.6 mm^3) for attenuation correction (AC), followed by a 15 min PET static emission scan, single bed position. All PET images on the PET/MR system were reconstructed using a standard, supplier-provided ordered subset expectation maximization (OSEM3D) algorithm with 4 iterations and 21 subsets, to yield 127 axial slices with pixel spacing 2.3 x 2.3 x 2.6 mm^3. Simultaneously, clinical routine breast MRI was performed with the following sequences: axial T2-weighted 2D-TSE sequence (described above with AF = 7) and a T1-weighted 3D-gradient echo sequence before and repeated four times after Gd-DTPA contrast agent injection (repeated at 90s, 180s, 270s, 360s pi with imaging parameters TR/TE 4.9 ms / 2.2 ms, FA 15°, bandwidth 360 Hz / pixel, TA 60s, matrix 352 x 350 x 160, pixel spacing 1.0 x 1.0 x 1.0 mm^3, acceleration factor 3). One patient was additionally scanned in our institute's standard clinical setting on a 3T MRI system (Ingenia 3.0T, Philips, Best, The Netherlands) with the 7-ch MR-only coil using the same MR imaging protocol.

Coil attenuation correction

To account for photon attenuation and scatter in the PET images due to the presence of the PET/MR coil, a CT-based AC- map of the coil was obtained [14] and added to the MR-acquired Dixon-based patient/phantom AC-map [13]. For this purpose a CT image of the coil was acquired on the PET/CT system with a tube voltage / current of 120 kV / 105 mA. The vendor (Siemens) -supplied MAR (Metal Artifact Reduction) reconstruction was used to reduce streaking artifacts. Conversion of Hounsfield units to linear attenuation coefficients for positron annihilation photons at 511 keV was achieved by bilinear mapping [14]. The coil AC-map was re-sampled to match the resolution of the MR-acquired patient AC-map (M_p). Co-registration of template coil map M_c and on-the-fly acquired patient/phantom map M_p was achieved by using a little marker (10-ml water filled vial), visible in both maps and integrated at a fixed position in the coil (yielding M_{pc}) (Fig. 1c). A single marker to determine the coil position along the head-foot dimension was sufficient for registration since the coil is in a fixed position along dimensions left-right and anterior-posterior by being placed on the patient table.

Data analysis

For MR performance evaluation coil sensitivity was assessed by generating SNR and noise correlation maps from the phantom and volunteer data and compared to the 16-ch MR-only coil.

Phantom Measurements

The effect of MR coil presence on PET data was first assessed by the overall PET photon count loss. This was measured by comparing total PET photon counts in the phantom emission experiment with and without the coil present in the FOV. Data were compared for the dedicated PET/MR coil and MR-only coils. Second, the ability to recover PET image homogeneity and accurate SUV quantification using the implementation of the CT-based coil AC was evaluated. To this end, PET images were reconstructed using AC for (i) phantoms only (M_p) and (ii) for phantoms and coil combined (M_{pc}). These images were normalized to a reference data set, which consisted of a PET acquisition without the coil present.

Human Measurements

In the patient studies, PET images from the PET/MR system were reconstructed i) without coil correction (M_p) and ii) using the combined AC-map M_{pc}. Images were judged qualitatively. Criteria for "good" image quality were lesion conspicuity and a homogeneous tracer distribution in the liver. Even though no true "gold standard" reference existed, quantitative lesion SUV were reported for M_p and M_{pc} reconstructed PET images. Volumes of interests (VOIs) were drawn around lesions, using a threshold of 50% of SUV_{max}. For further analysis, the VOI mean SUV values were used.

RESULTS

MR performance

As a measure for SNR performance, the noise correlation of the PET/MR breast coil yielded a mean [min, max] value of 0.068 [8.7e-4, 0.39]. Regional sensitivity is illustrated by the SNR map of the PET/MR coil and compared to the 16-ch MR-only coil in Fig. 2b. Profile plots through the phantom demonstrate the almost identical SNR in both coils (Fig. 2a). Also in vivo, the acquired SNR map yielded comparable appearance to the 16-ch MR-only coil (Fig. 2c,d). Overall MR image quality of the clinical protocol sequences in the PET/MR patient study was qualitatively comparable to the clinical routine MR-only study (Fig. 3).

PET performance

Phantom Measurements

In the PET emission experiment, the presence of the PET/MR coil caused only a 15% reduction in overall true counts compared to 20% for MR-only coils. Of the 15% PET photon reduction caused by the PET/MR coil presence, 8% were found to be caused by the coil housing and the remaining attenuation must be attributed to the electronic components. Neglecting the coil in the AC resulted in an underestimation of SUV, as well as an appearance of inhomogeneities in the phantom PET images, compared to the reference data acquired without the coil present (Fig. 4a). The reconstruction of PET images acquired with coil present, but using M_p only, yielded a mean SUV underestimation of 22%. The use of the combined AC-map M_{pc} recovered accurate SUV values and improved image homogeneity (Fig. 4b).

Human Measurements

Also in vivo, a qualitative improvement in visual image appearance was found after the coil was included in the AC-map. This is demonstrated in the PET images of Fig. 5 by the recovery of a homogeneous tracer distribution in the liver as well as the recovery of small lesion conspicuity. A comparison of all 14 analyzed lesions showed a high correlation between PET reconstructed with M_{pc} and with M_p ($R^2 = 0.99$, p-value < 0.001, Fig. 6a). Quantitative analysis showed that including the coil template in AC, i.e. using M_{pc} rather than M_p, resulted in an increase of SUV in the lesion VOIs (normalized difference: mean ± SD = 21 ± 9%, Fig. 6b). Even though mean SUV increased for all 14 lesions of the seven patients, the actual increase showed substantial variability among patients, ranging from 2% to 36% (Fig. 6b).

DISCUSSION

In clinical breast MRI, dedicated coils are commercially available as biopsy or diagnostic coils featuring between 4 and up to 16 receiver channels. We have chosen a 16-ch design to support fast and high quality diagnostic MRI. Our evaluation of signal sensitivity and overall image quality in phantoms and first patients showed, that using this coil, state-of-the-art breast MRI is possible in the setting of simultaneous PET/MR. A clear advantage of the 16-ch design was demonstrated by highly parallel image acquisition, which enabled a substantial reduction in image acquisition time without significant degradation in image quality.

In simultaneous PET operation, the presence of the MR coil in the PET FOV causes attenuation and scatter of 511 keV positron annihilation photons. Recently, results have been published showing implementation of a commercially available 4-ch breast

biopsy MR coil in simultaneous PET/MR [9,10]. Overall attenuation of PET photons caused by the presence of the 4-ch coil was reported as 11% [10]. In this study, we found for two MR-only breast coils with 7-ch and 16-ch designs 20% overall photon attenuation and 15% for the 16-ch PET/MR coil with electronics replaced outside of the PET line-of-response (LOR) space. Even though these results are important to characterize the effect of the specific MR coil presence on PET imaging, the overall attenuation within the range of these numbers is not a limiting factor for simultaneous PET/MR operation. More of a concern is the appearance of regional artifacts in PET images due to the attenuation and scatter caused by the presence of the MR coil [8,10,15]. Since these regional effects might coincide with lesion location, the quantification of lesion SUV might be significantly altered by the presence of the coil. Therefore, using the coil without any further correction clinically makes a huge difference. However, other groups already demonstrated that these effects could be corrected using a CT-based template map of the coil in PET image reconstruction [6,9,10]. Similar, in this study we acquired a CT-based template map of the coil, which was converted to attenuation values at the 511 keV photon energy by a standard bilinear mapping approach [14,16]. Using the template method, our results showed that SUV underestimation could be reduced from 22% to only 2% in phantom experiments. This result is well within limits found by other groups, e.g. the template AC approach implemented for the 4-ch MR-only breast coil by Aklan et al. yielded accurate SUV quantification within 5% [10].

In patients, the implementation of the coil template in the attenuation map yielded a substantial increase in lesion SUV for all patients (mean increase for all lesions = 21%). In addition we observed a large variability of the SUV correction for individual lesions (ranging from 2% to 36%), especially for lesions with a low SUV. This suggests that a simple bias correction is not sufficient, but rather the integration of the coil specific attenuation is mandatory in order to perform an optimal, patient specific reconstruction. One limitation of this study is that we did not compare our coil corrected lesion SUV values to a true “gold standard” reference. Even though such a comparison was obtained and validated in a phantom and similar SUV increase was observed in vivo, inhomogeneous in vivo tracer distribution, such as high activity coming from liver or myocardium, might influence the coil correction method.

CONCLUSION

We have developed and evaluated a 16-ch breast coil specifically designed for simultaneous PET/MR imaging. Our results showed that using this coil, state-of-the-art breast MRI was possible in the setting of simultaneous PET/MR. In quantitative PET imaging, using the coil without any further correction could alter lesion SUV quantification and therefore severely impact clinical operation. In a phantom this bias

could be largely corrected by using a CT-template map of the coil within the attenuation correction for PET image reconstruction, however in vivo the method needs further validation.

ACKNOWLEDGEMENTS

We gratefully acknowledge the excellent technical assistance of Sylvia Schachoff, Anna Winter and Claudia Meisinger (all TU München). We thank Rebekka Kraus (TU München), Christine Dörnfeld (Uni-Klinik Würzburg) and Siemens Healthcare for fruitful discussions.

This study has received funding by the „Bundesministerium für Wirtschaft und Technologie (BMWi)“ (German Ministry of Economics and Technology, ZIM-Kooperationsprojekte KF2922301RR1). The PET/MR system used for this study was funded through the “Deutsche Forschungsgemeinschaft (DFG) Grossgeräteinitiative 2010”. This work was supported in part by a research grant from Siemens Healthcare.

REFERENCES

1. Pichler BJ, Judenhofer MS, Catana C, et al. Performance test of an LSO-APD detector in a 7-T MRI scanner for simultaneous PET/MRI. *J Nucl Med*. 2006 Apr;47(4):639-47.
2. Catana C, Procissi D, Wu Y, et al. Simultaneous in vivo positron emission tomography and magnetic resonance imaging. *Proc Natl Acad Sci U S A*. 2008 Mar 11;105(10):3705-10.
3. Judenhofer MS, Wehrl HF, Newport DF, et al. Simultaneous PET-MRI: a new approach for functional and morphological imaging. *Nat Med.* 2008 Apr;14(4):459-65.
4. Catana C, Wu Y, Judenhofer MS, Qi J, Pichler BJ, Cherry SR. Simultaneous acquisition of multislice PET and MR images: initial results with a MR-compatible PET scanner. *J Nucl Med*. 2006 Dec;47(12):1968-76.
5. Mann RM, Kuhl CK, Kinkel K, Boetes C. Breast MRI: guidelines from the European Society of Breast Imaging. *Eur Radiol*. 2008 Jul;18(7):1307-18.
6. Delso G, Martinez-Möller A, Bundschuh RA, Ladebeck R, Candidus Y, Faul D, Ziegler SI. Evaluation of the attenuation properties of MR equipment for its use in a whole-body PET/MR scanner. *Phys Med Biol*. 2010 Aug 7;55(15):4361-74.
7. Tellmann L, Quick HH, Bockisch A, Herzog H, Beyer T. The effect of MR surface coils on PET quantification in whole-body PET/MR: results from a pseudo-PET/MR phantom study. *Med Phys*. 2011 May;38(5):2795-805.

8. Paulus DH, Braun H, Aklan B, Quick HH. Simultaneous PET/MR imaging: MR-based attenuation correction of local radiofrequency surface coils. *Med Phys*. 2012 Jul;39(7):4306-15.
9. Bowen SL, Seethamraju RT, Niell BL, Catana C. Optimization of MR and PET image quality for breast imaging with the Biograph mMR. [abstract] *Proc Intl. Soc Magn Reson. Med 20* 2012, p. 3009.
10. Aklan B, Paulus DH, Wenkel E, et al. Toward simultaneous PET/MR breast imaging: Systematic evaluation and integration of a radiofrequency breast coil. *Med Phys.* 2013 Feb;40(2):024301.
11. Wichmann T, Kurth R, Gepper C, et al. A 16 Channel Phased Array Coil Optimized for Diagnostic Breast Imaging. [abstract] *Proc Intl. Soc Magn Reson. Med 17* 2009, p. 3427.
12. Kellman P, McVeigh ER. Image reconstruction in SNR units: a general method for SNR measurement. *Magn Reson Med.* 2005 Dec;54(6):1439-47. Erratum in *Magn Reson Med.* 2007 Jul;58(1):211-2.
13. Martinez-Möller A, Souvatzoglou M, Delso G, et al. Tissue classification as a potential approach for attenuation correction in whole-body PET/MRI: evaluation with PET/CT data. *J Nucl Med*. 2009 Apr;50(4):520-6.
14. Burger C, Goerres G, Schoenes S, Buck A, Lonn AH, Von Schulthess GK. PET attenuation coefficients from CT images: experimental evaluation of the transformation of CT into PET 511-keV attenuation coefficients. *Eur J Nucl Med Mol Imaging.* 2002 Jul;29(7):922-7.
15. Tellmann L, Quick HH, Bockisch A, Herzog H, Beyer T. The effect of MR surface coils on PET quantification in whole-body PET/MR: results from a pseudo-PET/MR phantom study. *Med Phys.* 2011 May;38(5):2795-805.
16. Kinahan PE, Hasegawa BH, Beyer T. X-ray-based attenuation correction for positron emission tomography/computed tomography scanners. *Semin Nucl Med*. 2003 Jul;33(3):166-79.

FIGURES

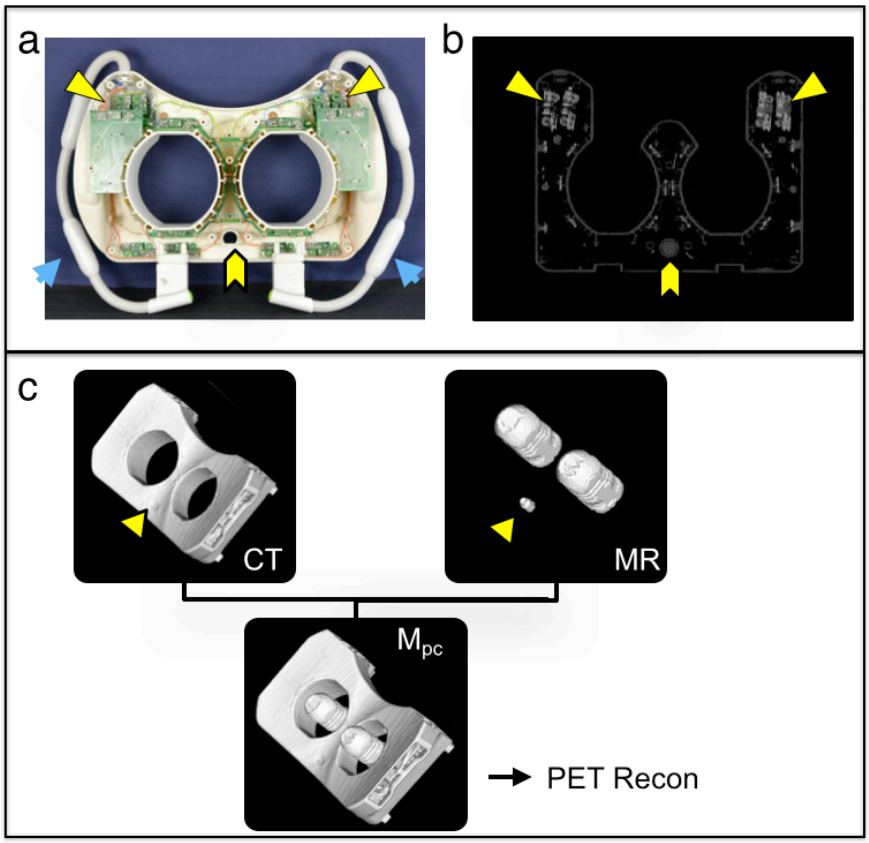

Figure 1: Design and implementation of the dedicated PET/MR breast coil. Optimizations for PET performance are illustrated by a photograph of coil electronics (a) and the corresponding attenuation correction (AC)-map (b). Note that the plugs in Fig. 1a are shown in storage position (blue arrows); once plugged in, they are outside of the axial PET imaging FOV and therefore do not contribute to photon attenuation.

Implementation of CT-template based attenuation correction shown in Fig. 1c. The CT-acquired coil map M_c and the MR-acquired phantom map M_p were combined to M_{pc}, using the MR visible marker indicating the coil position in M_p. The resulting combined map M_{pc} is used for attenuation correction in the PET image reconstruction algorithm.

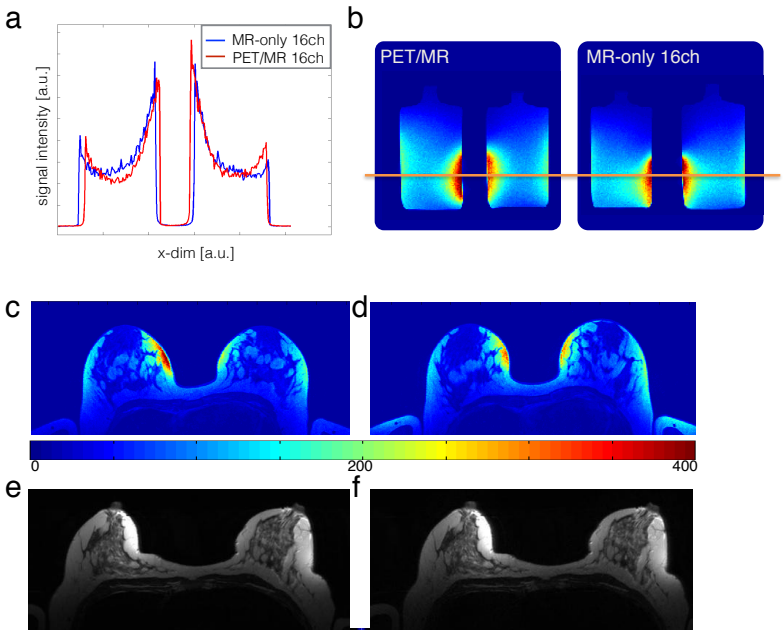

Figure 2: MR evaluation of the PET/MR coil. SNR profiles (shown in (a), position indicated by orange lines in (b) of a phantom MR acquisition showed the typical surface coil sensitivity pattern of high-element phased array coils: high sensitivity close to the coil elements, which decreased with increasing distance from the coil elements. The PET/MR coil sensitivity profile (red curve in (a)) was found to be identical to the 16-ch MR-only coil (blue curve in (a)). Corresponding SNR maps are shown in (b).

SNR scaled images of healthy volunteer scan using the PET/MR coil (c) and the 16-ch MR-only coil (d) showed qualitatively similar SNR performance. To demonstrate parallel imaging performance, a healthy volunteer was scanned twice using the 16-ch PET/MR breast coil with acceleration factor AF = 3 (e) and AF = 7 (f) in T2-weighted TSE MRI (phase encoding (PE) right-left, resolution PE = 384, reference lines 33 for AF 3 and 39 for AF 7). The 16-channel coil design supported high acceleration factors with a substantial reduction in acquisition time (7 min 23 s with AF = 3 reduced to 4 min 17 s with AF = 7), while no image artifacts were observed.

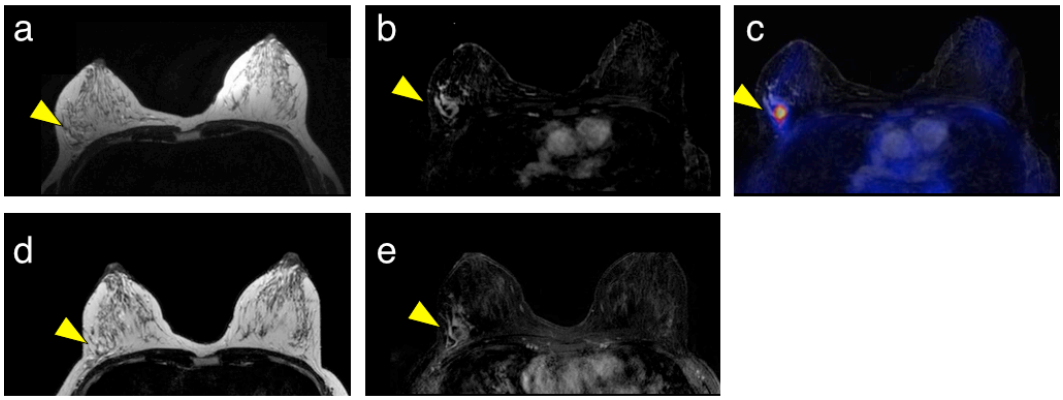

Figure 3: First in vivo results of simultaneous PET/MR in a breast cancer patient using the dedicated PET/MR breast coil. MR image quality in simultaneous PET/MR (T2w TSE sequence without fat suppression in (a), T1w dynamic 3D acquisition with subtraction of images post – pre Gd-DTPA contrast agent administration in (b) was comparable to the clinical standard exam (T2w TSE in (d), and T1w subtraction images in (e), both acquired on a Philips 3T MRI system with a 7-ch MR-only coil). The additional value of simultaneous PET is illustrated in (c), showing vivid ^{18}F-FDG uptake in the lesion.

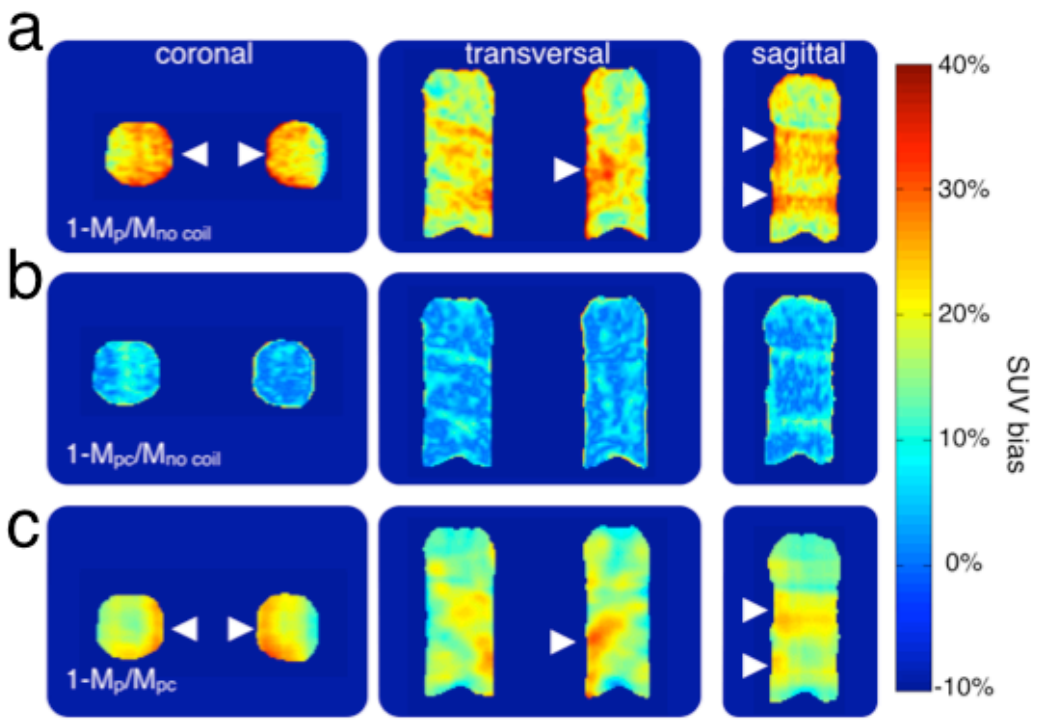

Figure 4: PET phantom images showed substantial overall and regionally varying SUV underestimation (white arrows in (a)), if coil was present, but no coil attenuation correction (AC) was used ((a) with M_p) with substantial improvement after coil AC was included ((b) with M_{pc} „no MAR“) compared to „no coil“ reference data. Correction of tracer uptake by implementing the coil in the AC mainly occurred in areas close to the coil (white arrows in (c) showing the relative changes in SUV if using M_{pc} rather than M_p).

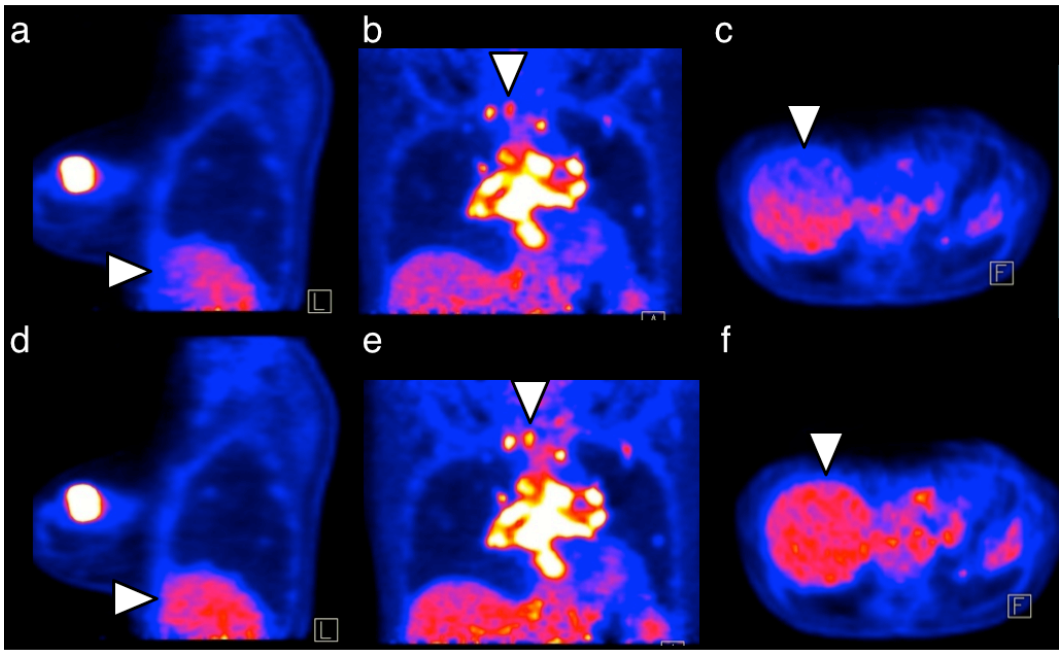

Figure 5: In vivo PET images showing effect of inclusion of attenuation correction for coil. PET image reconstruction using patient u-map only shown in (a-c) exhibit loss of signal intensity in liver from posterior towards anterior (closer to coil) in the liver (white arrows in a,c). This artifact is corrected by using the coil-patient combined u-map (d-f). Especially in small lesions the effect of including the coil attenuation correction can result in a conspicuous increase in lesion tracer activity (white arrow in b and e).

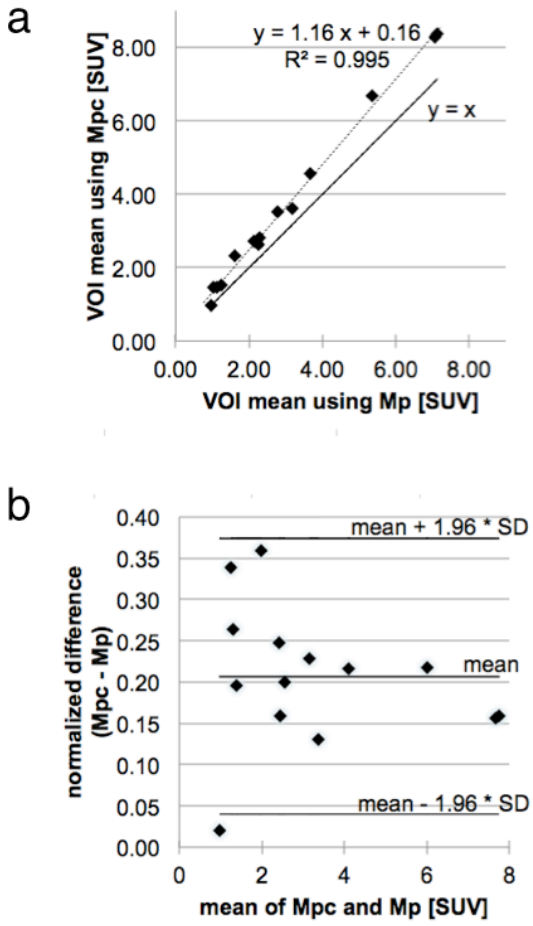

Figure 6: PET SUV using patient and coil combined AC map (Mpc) versus PET image reconstruction using only patient AC map (Mp) (Fig. 6a). Shown are the VOI mean values of 14 lesions in seven patients (with PET/MR breast coil in prone position) (Fig. 6a). Modified Bland-Altman-Diagram (Fig. 6b) shows normalized difference vs. mean PET SUV in lesions using patient only (Mp) and using patient and coil combined AC map (Mpc). Lines were drawn for mean bias (21%) as well as limits of agreement, which are given by mean ± 1,96* standard deviation (upper limit: mean bias +1,96*SD = 37%; lower limit: mean value – 1,96* SD = 4%).